# CrystEngComm

Accepted Manuscript

ROYAL SOCIETY OF CHEMISTRY

www.rsc.org/crystengcomm

Journal Name

COMMUNICATION

# Halogen bonding influences perylene-core twists in non-core substituted perylene tetraesters

Received 00th January 20xx,
Accepted 00th January 20xx

DOI: 10.1039/x0xx00000x

www.rsc.org/

Jonathan P. Wojciechowski,[a,b] Adam D. Martin,[a,b] Mohan Bhadbhade,[a,c] James E. A. Webb[a,b] and Pall Thordarson*[a,b]

**Halogen bonding has emerged as a popular synthon in supramolecular architectures. Its effects on supramolecular perylene systems however has been under investigated. We report X···O halogen bonding of perylene-3,4,9,10-tetracarboxylic tetra esters. This templates a twisted perylene core which affects its spectral properties. We show this interaction exists in both the solution and solid state through spectroscopy studies and single crystal analysis.**

Perylenes have been utilised in a broad range of applications such as: luminescent solar concentrators,[1] light harvesting scaffolds,[2] model supramolecular systems[3] and fluorescence spectroscopy.[4] This is largely due to their unmatched chemical versatility which allows for the tuneable construction of novel supramolecular architectures. It has been demonstrated that control of these supramolecular architectures is essential to the rational design of perylene-derived functional materials.[5]

Supramolecular self-assembly strategies of perylenes generally include; π-π stacking, metal coordination, hydrogen bonding and van der Waals interactions.[6] The use of halogen bonding in the construction of supramolecular assemblies has emerged as a powerful tool however has been under represented in the supramolecular assembly of perylene derivatives, with only one example in reported literature.[7] It is known that halogens can act as halogen bond (XB) donors through a phenomena known as the σ-hole effect and as a result, lone pairs of electrons can act as XB acceptors.[8,9] This follows a trend of I>Br>Cl>F in terms of XB donor strength. Nitrogen containing heterocycles are most commonly employed as XB acceptors, however carbonyl groups are also used. Nitrogen containing heterocycles form monotopic halogen bonds, which are limited to one dimensional arrays of halogen bonds. Oxygen can accept two halogen bonds to form a pairwise interaction and presents an interesting synthon for the construction of two and three dimensional supramolecular architectures. As a result, a number of supramolecular systems have been designed around this motif.[10-16]

Herein we report both monotopic and pairwise halogen bonding of a perylene tetraester with halogenated solvents (Scheme. 1). To our knowledge this is the first example of halogen bonding to a non-core substituted perylene derivative. Halogen bonding here acts as a template to give a twisted perylene core which is seldom observed in non-core substituted perylenes.[17] As a result, the spectral properties of the perylenes are affected by the degree of torsion. We use Hirshfeld surface analysis[18] to visualise the effects of solvent inclusion and halogen bonding within these perylene tetraester structures, which allows for quick and easy identification of the unique halogen bonding interactions and resulting changes in perylene stacking present in the solvates. Further, we demonstrate this interaction exists in solution through fluorescence spectroscopy and measure its binding constant using $^1$H NMR titrations fitted to 1:1 and statistical 1:2 binding models.

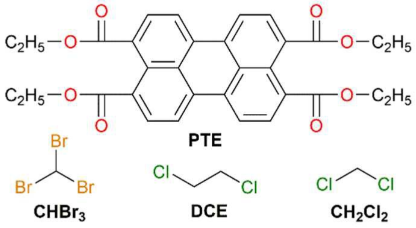

**Scheme. 1** Perylene-3,4,9,10-tetracarboxylic tetraethyl ester and its co-crystallised halogenated solvents

Perylene-3,4,9,10-tetracarboxylic tetraethyl ester (PTE) was synthesised via ring opening and alkylation of perylene-3,4,9,10-tetracarboxylic dianhydride using well established procedures to give the tetra ester in 71% yield.[19] The tetraethyl ester (PTE) crystallises from THF/ethanol in the

---

[a] School of Chemistry, The University of New South Wales, Sydney, 2052, NSW, Australia. E-mail: p.thordarson@unsw.edu.au
[b] The Australian Centre for Nanomedicine and the ARC Centre of Excellence for Convergent Bio-Nano Science and Technology, The University of New South Wales, Sydney, 2052, NSW, Australia.
[c] Mark Wainwright Analytical Centre, The University of New South Wales, Sydney, 2052, NSW, Australia.

Electronic Supplementary Information (ESI) available: See for experimental methods including synthesis of PTE, methods for obtaining single crystals, Hirshfeld analysis, and binding studies. See DOI:10.1039/x0xx00000x triclinic $P\overline{1}$ space group, with this structure previously reported incorrectly in the literature[19] in space group P1 with two full independent molecules in the unit cell. The solvent free crystal structure (PTE) contains two half PTE molecules, each lying about independent inversion centres. The dichloromethane solvate (PTE·CH$_2$Cl$_2$) also crystallises in this space group ($P\overline{1}$) from CH$_2$Cl$_2$/hexane and also contains two half PTE molecules each lying about independent inversion centres with one CH$_2$Cl$_2$ in a general position. Whereas the 1,2-dichloroethane (PTE·DCE), crystallises from DCE/hexane and pack into the monoclinic C2/c space group with PTE lying about an inversion centre with 1,2-dichloroethane disordered about a two-fold axis. The bromoform solvates (PTE·2(CHBr$_3$)) crystallises from pure CHBr$_3$ in an orthorhombic Pna$_{21}$ space group with one PTE in the asymmetric unit and two CHBr$_3$ molecules in general positions. Single crystal analysis reveals X···O halogen bond interactions for the dichloromethane (PTE·CH$_2$Cl$_2$) and bromoform (PTE·2(CHBr$_3$)) solvates. The bromoform solvate (PTE·2(CHBr$_3$)) displays a pairwise interaction between the tetraester carbonyl to the bromoform (C=O···Br = 2.787(5)-3.032(5) Å and ∠C=O···Br = 158-173°), (Fig. 1).

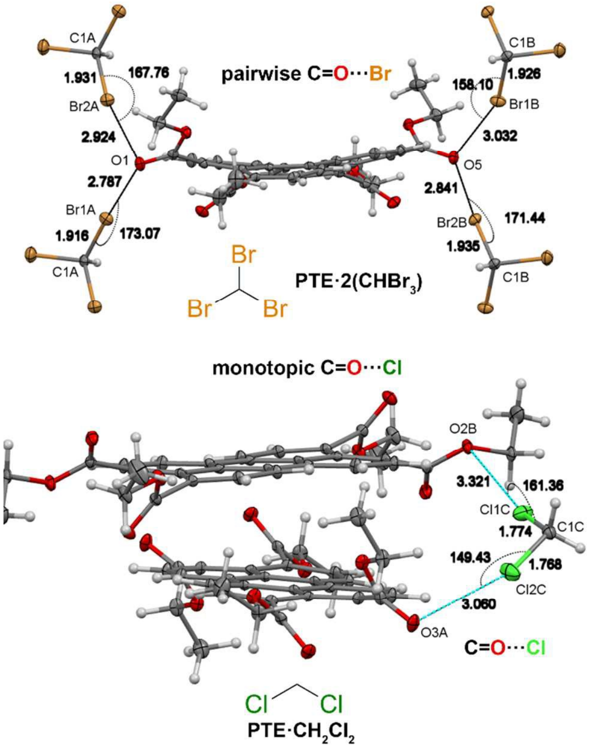

**Fig. 1** Pairwise C=O···Br carbonyl interaction found in the PTE·2(CHBr$_3$) solvate compared to the monotopic C=O···Cl and C-O···Cl interactions found in the PTE·CH$_2$Cl$_2$ solvate. The carbonyl oxygen in the bromoform solvate forms two halogen bonds to the bromoform whereas the dichloromethane solvate only forms one halogen bond to each dichloromethane.

After careful survey of the Cambridge structural database (CSD), the C=O···Br bond distance is among the shortest reported.[20] Furthermore, a ∠C=O···Br ≈ 180° is evidence for a very strong halogen bond interaction. Halogen bonding is also evident for the dichloromethane included structure (PTE·CH$_2$Cl$_2$), however in comparison to PTE·2(CHBr$_3$) which shows a pairwise interaction, PTE·CH$_2$Cl$_2$ displays monotopic C=O···Cl and C-O···Cl interactions with distances of 3.060(13) Å and 3.321(14) Å respectively and ∠C=O···Cl = 149, ∠C-O···Cl = 161°. The decrease in ∠C=O···Cl compared to ∠C=O···Br is most likely due to the decreased bond strength of Cl as a XB donor compared to Br. Compared to PTE·CH$_2$Cl$_2$, the C=O···Cl bond distance in PTE·DCE is 3.598(5) Å which exceeds the sum of the van der Waals radii. It should be noted however that due to the disorder in the 1,2-dichloroethane included structure, any potential halogen bonding interactions were difficult to quantify.

In addition to the C=O···Br interactions of PTE·2(CHBr$_3$), there are also aryl C-H···Br interactions with distances of 3.042-3.048 Å which occur at the 2 and 11 positions of the perylene. This aryl C-H···Br interaction is likely templated cooperatively through the formation of the pairwise C=O···Br interactions, which allow this close interaction to occur. In addition, PTE·CH$_2$Cl$_2$ also displays an aryl C-H···Cl interaction with an increase distance of 3.396-3.582 Å. As a result, bromoform and dichloromethane alter the torsion of the perylene core which is otherwise planar in the solvent-free structure (PTE) (Fig. 2 and Table. 1).

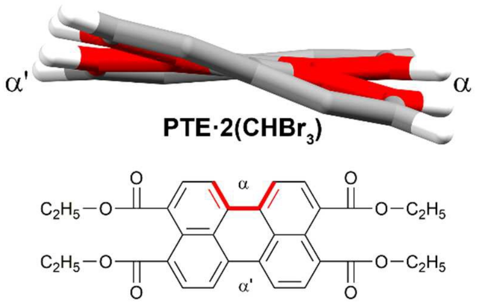

**Fig. 2** Torsion of the perylene-core in PTE·2(CHBr$_3$) as a result of C=O···Br halogen bonding and aryl C-H···Br interactions. Ester groups have been omitted from the structure for clarity.

**Table. 1** Measured torsion angles of the crystal solvates obtained in this study.

| Crystal Structure | trans conformer [a] | | cis conformer [a] | |
|---|---|---|---|---|
| | α | α′ | α | α′ |
| **PTE** | 0.91° | -0.91° | 0.16° | -0.16° |
| **PTE·DCE** | - | - | 0.73° | 0.73° |
| **PTE·CH$_2$Cl$_2$** | 1.59° | -1.59° | 3.25° | -3.25° |
| **PTE·2(CHBr$_3$)** | - | - | -11.57° | -10.24° |

[a] PTE and PTE·CH$_2$Cl$_2$ contain two perylenes in the unit cell. They are defined as either the *cis* or *trans* conformer respectively by the orientation of the esters groups. See Fig. S1, ESI† for more details.

PTE·CH$_2$Cl$_2$ displays torsion angles of 1.59° and 3.25° whereas PTE·2(CHBr$_3$) contains larger torsion angles of 10.2° and 11.6°. This difference in torsion angle of the solvates is in agreement with the aryl C···H-X distances found through crystal analysis. In comparison, the solvent-free structure and 1,2-dichloroethane solvate both have torsion angles less than 1°. A planar core is common for non-substituted perylenes, and generally only bay or ortho substitution of the perylene results in torsional twists.[21]

It has been shown in studies with bay-substituted perylenes, core torsion reduce π-π interactions.[22] We find this to also be the case when comparing the various solvates using Hirshfeld surface and analysing the fingerprint plot generated.[18] Contact distances for various intermolecular interactions can be measured from the sum of $d_e$ and $d_i$ values, which represent the positions of atoms exterior and interior to the generated Hirshfeld surface respectively. Close interactions are shown on the generated surface as red points and represent interactions less than the sum of the van der Waals radii.

The solvent-free structure (PTE) features multiple close π-π interactions between the perylene cores (C⋯C = 3.21(2) Å) and hydrogen bonding between the ester carbonyls and ester methylene groups of adjacent perylenes. These interactions are confirmed through analysis of the Hirshfeld surface and also appear as sharp peaks in the fingerprint plot (see Fig. S2, ESI†). Similar interactions are found for the 1,2-dichloroethane solvate (PTE·DCE) which shows no halogen bonding. This observation is consistent with the crystal analysis and confirmed in the fingerprint plot, which show no sharp peaks for C=O⋯Cl or C-O⋯Cl interactions. The fingerprint plot is similar compared to the solvent free structure however structurally 1,2-dichloroethane molecules pack in channels around the perylene tetraester (see Fig. S3, ESI†), resulting in a change of space group. This is also accompanied by a small increase in the π-π distance (C⋯C = 3.26(3) Å). For the solvates which display halogen bonding, PTE·$CH_2Cl_2$ and PTE·2($CHBr_3$), sharp peaks in the fingerprint plot clearly indicate the presence of C=O⋯X and C-O⋯X halogen bond interactions. The solvates have increased π-π distances (C⋯C = 3.30(2) Å and C⋯C = 3.53(8) Å for PTE·$CH_2Cl_2$ and PTE·2($CHBr_3$) respectively, see Fig. S4 and S5, ESI†). This follows a trend where as halogen bond strength increases, π-π interactions decrease and this is likely brought about by the increase in torsion angle. Furthermore, there is a type I Br⋯Br interaction (where ∠C-X⋯X' = ∠C-X'⋯X) between adjacent bromoform molecules.[9]

It has been shown that the packing of perylene derivatives due to their strong π-π interactions greatly affect their photophysical and electron transport properties.[23] Therefore the torsional twist of the perylene core, should give a change in the fluorescence spectra if this interaction exists in solution. Interestingly, upon dissolution of PTE into bromoform the emission band and excitation of perylene tetraester is bathochromically shifted (Fig. 3). We use tetrahydrofuran (THF) as a reference solvent as it solvates PTE without halogen bonding. The excitation band of PTE is shifted bathochromically 9 nm in bromoform in reference to THF. This is further exemplified in the emission bands, with a large bathochromic shift of 12 nm for bromoform. Smaller bathochromic shifts (6 nm) of the emission spectra are found for dichloromethane which displays a smaller torsional twist of the perylene core. Furthermore, 1,2-dichloroethane and THF have identical emission and excitation profiles which agrees with their torsion angles of < 1°. This suggests the bathochromic shift of the fluorescence emission is affected by the degree of torsion, where a larger torsion is accompanied by a greater shift in fluorescence emission. The inclusion of halogen bonding does not directly alter the spectral properties of the perylenes, instead it indirectly affects the packing of the perylene, which then changes the spectral properties through core torsion.

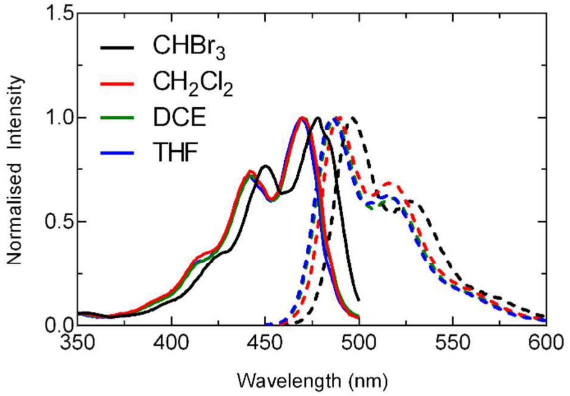

**Fig. 3** Normalised fluorescence spectroscopy of PTE in various solvents. Excitation at 400 nm and emission at 550 nm. The excitation spectra of PTE in bromoform is shifted bathochromically 9 nm in reference to THF whereas the emission spectra of PTE in bromoform is bathochromically shifted 12 nm in reference to THF. Dichloromethane shows a small 6 nm bathochromic shift in the emission spectra. 1,2-dichloroethane (DCE) and THF show similar emission and excitation spectra.

We employed $^1H$ NMR titrations to investigate the binding constant associated with this spectral shift. $^1H$ NMR titrations reveal a small shift of the perylene 1,6,7,12 H-resonances and 2,5,8,11 H-resonances upon titration with bromoform (see Fig. S6, ESI†). We fitted these shifts using a 1:1 and statistical 1:2 binding models (where host concentration is doubled then fitted to a 1:1 model) using Bindfit[24] which is based on previously published binding programs.[25] The 1:1 binding model gives a K = 8.51 ± 0.93 $M^{-1}$ whereas the statistical 1:2 gives a K = 8.65 ± 0.96 $M^{-1}$. Comparing covariance and errors, both models fit equally well. We have shown this also to be the case in our previous studies and was further elucidated through single crystal analysis and DFT calculations.[26] From the crystal structure unit cell, we can see PTE·2($CHBr_3$) is in agreement with the statistical 1:2 binding model, containing one perylene unit and two bromoform molecules. Furthermore, the $^1H$ NMR titration is in agreement with the crystal structure of PTE·2($CHBr_3$) which show a greater shift of the more affected 1,2,7,12 H-resonances and smaller shifts of the 2,5,8,11 H-resonances which are less affected.

We have reported the first example of X⋯O halogen bonding to a non-core substituted perylene tetraester in both the solid and solution state. Presented in this work is single crystal evidence for C=O⋯Cl, C-O⋯Cl and the less common pairwise C=O⋯Br halogen bond interaction. These interactions influence the π-π stacking of the perylene cores, packing of the ester groups and even the torsion of a non-core substituted perylene. Interestingly, fluorescence spectroscopy of the perylene tetra ester indicates that these halogen bond interactions also exist in the solid state, and indirectly result in a bathochromic shift of the fluorescence spectra through a torsion of the perylene core in the bromoform solvate. $^1$H NMR experiments confirm the core-torsion of the bay positions (1,2,7,12) of the perylene. We find this interaction fits to a statistical 1:2 binding model which is in agreement with the crystal structure. This work clearly demonstrates the interplay between halogen bonding and π-π interactions in highly conjugated systems such as perylenes and has important implications for the future rational design of functional supramolecular architectures based upon halogen bonds.

We would like to thank the Mark Wainwright Analytical Centre (UNSW) for access to instruments. We acknowledge the Australian Research Council for Discovery Project Grant (DP130101512), an ARC Centre of Excellence Grant (CE140100036) and a Future Fellowship to PT (FT120100101) and the Australian Government for PhD scholarships to JPW. We would also like to thank Dr. Jonathon E. Beves for his comments on the manuscript.

## Notes and references

Crystal data for **PTE**: $C_{32}H_{28}O_8$, $M$ = 540.54, triclinic $P\bar{1}$ (No. 2), $a$ = 7.5230(15), $b$ = 11.901(2), $c$ = 15.487(3), $\alpha$ = 107.50(3), $\beta$ = 101.49(3), $\gamma$ = 96.92(3), $V$ = 1271.5(5) Å$^3$, $Z$ = 2, T = 100 K, $D_{calcd}$ = 1.412 gcm$^{-3}$, $\mu$ = 0.102 mm$^{-1}$, $N$(unique) = 4630 (merged from 5588), $R_{int}$ = 0.0636, $R_1$ = 0.0527, $wR_2$ (all data) = 0.1349, GOF = 1.038, max $\Delta F$ peak = 0.370 e Å$^{-3}$ CCDC Number: 1468083

Crystal data for **PTE·CH$_2$Cl$_2$**: $C_{33}H_{30}Cl_2O_8$, $M$ = 625.47, triclinic $P\bar{1}$ (No. 2), $a$ = 7.4880(15), $b$ = 13.035(3), $c$ = 15.569(3), $\alpha$ = 105.68(3), $\beta$ = 101.80(3), $\gamma$ = 90.67(3), $V$ = 1428.6(6) Å$^3$, $Z$ = 2, T = 100 K, $D_{calcd}$ = 1.454 gcm$^{-3}$, $\mu$ = 0.282 mm$^{-1}$, $N$(unique) = 6840 (merged from 7572), $R_{int}$ = 0.0541, $R_1$ = 0.0505, $wR_2$ (all data) = 0.1346, GOF = 1.069, max $\Delta F$ peak = 0.677 e Å$^{-3}$ CCDC Number: 1468082

Crystal data for **PTE·DCE**: $C_{34}H_{32}Cl_2O_8$, $M$ = 639.48, monoclinic C2/c (No. 15), $a$ = 26.689(5), $b$ = 15.869(3), $c$ = 7.1690(14), $\alpha = \gamma$ = 90, $\beta$ = 101.83(3), $V$ = 2971.7(11) Å$^3$, $Z$ = 4, T = 100 K, $D_{calcd}$ = 1.420 gcm$^{-3}$, $\mu$ = 0.272 mm$^{-1}$, $N$(unique) = 3590 (merged from 4368), $R_{int}$ = 0.1024, $R_1$ = 0.0884, $wR_2$ (all data) = 0.2488, GOF = 1.768, max $\Delta F$ peak = 1.014 e Å$^{-3}$ CCDC Number: 1468084

Crystal data for **PTE·2(CHBr$_3$)**: $C_{34}H_{30}Br_6O_8$, $M$ = 1046.04, orthorhombic Pna2$_1$ (No. 33), $a$ = 7.3120(15), $b$ = 23.629(5), $c$ = 20.889(4), $\alpha = \beta = \gamma$ =90, $V$ = 3609.1(13) Å$^3$, $Z$ = 4, T = 100 K, $D_{calcd}$ = 1.925 gcm$^{-3}$, $\mu$ = 6.724 mm$^{-1}$, $N$(unique) = 10341 (merged from 10581), $R_{int}$ = 0.0506, $R_1$ = 0.0498, $wR_2$ (all data) = 0.1304, GOF = 1.047, max $\Delta F$ peak = 1.199 e Å$^{-3}$ CCDC Number: 1468085

1 G. D. Gutierrez, I. Coropceanu, M. G. Bawendi and T. M. Swager, *Adv Mater*, 2016, **28**, 497-501.
2 S. T. Ryan, R. M. Young, J. J. Henkelis, N. Hafezi, N. A. Vermeulen, A. Hennig, E. J. Dale, Y. Wu, M. D. Krzyaniak, A. Fox, W. M. Nau, M. R. Wasielewski, J. F. Stoddart and O. A. Scherman, *J Am Chem Soc*, 2015, **137**, 15299-15307.
3 C. Roche, H. J. Sun, P. Leowanawat, F. Araoka, B. E. Partridge, M. Peterca, D. A. Wilson, M. E. Prendergast, P. A. Heiney, R. Graf, H. W. Spiess, X. Zeng, G. Ungar and V. Percec, *Nat Chem*, 2016, **8**, 80-89.
4 A. S. Weingarten, R. V. Kazantsev, L. C. Palmer, M. McClendon, A. R. Koltonow, A. P. Samuel, D. J. Kiebala, M. R. Wasielewski and S. I. Stupp, *Nat Chem*, 2014, **6**, 964-970.
5 F. Wurthner, T. E. Kaiser and C. R. Saha-Moller, *Angew Chem Int Ed Engl*, 2011, **50**, 3376-3410.
6 F. Wurthner, C. R. Saha-Moller, B. Fimmel, S. Ogi, P. Leowanawat and D. Schmidt, *Chem Rev*, 2016, **116**, 962-1052.
7 Y. Kumar, S. Kumar, S. Kumar Keshri, J. Shukla, S. S. Singh, T. S. Thakur, M. Denti, A. Facchetti and P. Mukhopadhyay, *Org Lett*, 2016, **18**, 472-475.
8 L. C. Gilday, S. W. Robinson, T. A. Barendt, M. J. Langton, B. R. Mullaney and P. D. Beer, *Chem Rev*, 2015, **115**, 7118-7195.
9 G. Cavallo, P. Metrangolo, R. Milani, T. Pilati, A. Priimagi, G. Resnati and G. Terraneo, *Chem Rev*, 2016, **116**, 2478-2601.
10 D. S. Yufit, R. Zubatyuk, O. V. Shishkin and J. A. K. Howard, *CrystEngComm*, 2012, **14**, 8222.
11 F. Bertolotti, G. Cavallo, P. Metrangolo, S. K. Nayak, G. Resnati and G. Terraneo, *Supramol. Chem*, 2013, **25**, 718-727.
12 J. N. Moorthy, P. Venkatakrishnan, P. Mal, S. Dixit and P. Venugopalan, *Cryst. Growth Des*, 2003, **3**, 581-585.
13 J.-L. Syssa-Magalé, K. Boubekeur and B. Schöllhorn, *J. Mol. Struct.*, 2005, **737**, 103-107.
14 A. Takemura, L. J. McAllister, S. Hart, N. E. Pridmore, P. B. Karadakov, A. C. Whitwood and D. W. Bruce, *Chem. Eur. J.*, 2014, **20**, 6721-6732.
15 H. S. El-Sheshtawy, B. S. Bassil, K. I. Assaf, U. Kortz and W. M. Nau, *J Am Chem Soc*, 2012, **134**, 19935-19941.
16 V. Vasylyeva, S. K. Nayak, G. Terraneo, G. Cavallo, P. Metrangolo and G. Resnati, *CrystEngComm*, 2014, **16**, 8102-8105.
17 Z. H. Zhang, J. L. Wang, N. Gao and M. Y. He, *Acta Crystallogr C Struct Chem*, 2014, **70**, 668-671.
18 M. A. Spackman and D. Jayatilaka, *CrystEngComm*, 2009, **11**, 19-32.
19 I. Seguy, P. Jolinat, P. Destruel, R. Mamy, H. Allouchi, C. Courseille, M. Cotrait and H. Bock, *ChemPhysChem*, 2001, **2**, 448-452.
20 I. J. Bruno, J. C. Cole, J. P. M. Lommerse, R. S. Rowland, R. Taylor and M. L. Verdonk, *J. Comput. Aided Mol. Des.*, 1997, **11**, 525-537.
21 P. Osswald and F. Wurthner, *J Am Chem Soc*, 2007, **129**, 14319-14326.
22 R. Schmidt, J. H. Oh, Y. S. Sun, M. Deppisch, A. M. Krause, K. Radacki, H. Braunschweig, M. Konemann, P. Erk, Z. Bao and F. Wurthner, *J Am Chem Soc*, 2009, **131**, 6215-6228.
23 Y. Yamamoto, T. Fukushima, Y. Suna, N. Ishii, A. Saeki, S. Seki, S. Tagawa, M. Taniguchi, T. Kawai and T. Aida, *Science*, 2006, **314**, 1761-1764.
24 www.supramolecular.org, (accessed 15th February, 2016).
25 P. Thordarson, *Chem Soc Rev*, 2011, **40**, 1305-1323.
26 E. N. Howe, M. Bhadbhade and P. Thordarson, *J Am Chem Soc*, 2014, **136**, 7505-7516.